Methane Elimination from Ionized Propane through an Ion−Neutral Complex: An ab Initio Study

Santiago Olivella,*,‡,§ Albert Solé,‡ and David J. McAdoo⊥

Contribution from the Departaments de Química Orgànica i Química Física, Universitat de Barcelona, Martí i Franquès 1, 08028 Barcelona, Catalunya, Spain, and the Marine Biomedical Institute, University of Texas Medical Branch, Galveston, Texas 77555-1069

Received February 26, 1996[⊗]

Abstract: In connection with the major unimolecular decompositions of ionized propane, namely, methane elimination and methyl radical loss, ab initio molecular orbital calculations at the UMP2/6-31G(d) (molecular geometries) and QCISD(T)/6-311+G(2d,2p) (energies) levels of theory have been used to investigate the relevant parts of the $C_3H_8^{\bullet+}$ ground-state potential energy surface (PES). The calculations demonstrate that at internal energies about 15 kJ/mol below the thermochemical threshold for methyl radical loss, partial bond dissociation to an ion−neutral complex consisting of the methyl radical coordinated to the H-bridged ethyl cation and methane elimination therefrom both occur. The contours of the $C_3H_8^{\bullet+}$ ground-state PES are such that at the threshold for methane elimination the methyl radical partner of the complex is directed to the hydrogen atom it will abstract without being able to move freely around the ethyl cation partner. A higher energy configuration of the ion−neutral complex, lying about 11 kJ/mol below the threshold for simple dissociation, mediates the carbon skeletal rearrangement of the propane radical cation. The observed predominance of the methane losses involving terminal carbon atoms over those involving the central carbon atom are rationalized on the basis that such a degenerate rearrangement precedes the methane elimination.

Introduction

The unimolecular chemistry of ionized alkanes in the gas phase has been the subject of ongoing experimental and theoretical research. Extremely complex behavior is frequently observed, even for relatively small alkane radical cation species. One of the major reactions of alkane molecular ions is ejection of smaller alkanes. The alkanes ejected are composed of alkyl fragments formed at favorable cleavage points and a hydrogen atom from an adjacent carbon atom, sometimes after isomerization. This has often been regarded as a 1,2 elimination, which may or may not be concerted. At present, mechanistic details concerning the alkane elimination from ionized saturated hydrocarbons are not well established. In particular, uncertainty remains about the decomposition of one of the most heavily studied small alkane ions, the propane radical cation. Some 20 years ago propane and deuterium-labeled propane ions were studied using threshold photoelectron−photoion coincidence mass spectrometry (TPE-CPI MS) by Stockbauer and Inghram.[1] They found that, although ionized propane-*2,2*-$^2H_2$ loses predominantly CH_4, the eliminations of CH_3D and CH_2D_2 were not negligibly small. This result contrasted with an earlier analysis of Lifshitz and Shapiro based on metastable peaks which suggested that the only significant CH_4 elimination involves a methyl group and a hydrogen atom from the terminal carbon.[2] Wolkoff and Holmes reexamined the metastable spectrum of ionized propane-*2,2*-$^2H_2$ and found that the metastable peak for elimination of CH_4 was at least 250 times more intense than elimination of CH_3D or CH_2D_2, but the peak intensities *m*/*z* 30:29:28 were about 100:8:9 at 1 eV above threshold.[3] They proposed that the elimination reactions which involve deuterium atoms from the central carbon have a slightly higher activation energy and are therefore barely observable in the microsecond time frame. Derrick and co-workers[4] interpreted the very large isotope effects (CH_4:CH_3D:CH_2D_2 = 0.87:0.01:0.12) associated with eliminations of CH_4, CH_3D, and CH_2D_2 from ionized propane-*1,1,2,2*-$^2H_4$ in terms of a nonclassical transition state in which a hydrogen atom on a methyl group has been transferred to a neighboring C−C bond, forming a three-center bond. Subsequent TPE-CPI MS studies by Meisels and co-workers[5] indicated that approximately 11% of all methanes lost from ionized propane-*2*-^{13}C contain the central carbon atom and that the threshold energies for methane losses involving terminal and central carbon atoms lie within 0.22 eV of each other. They proposed that carbon skeletal rearrangement of the propane molecular ion does not precede fragmentation leading to the loss of methane, but that loss of the center carbon atom may occur in a concerted stepwise cleavage involving a transition state tighter than that for methane loss involving the terminal carbon atoms.

We recently reported[6] a theoretical study showing that methane elimination from both ionized butane and isobutane is mediated by ion−neutral complexes, i.e., species in which noncovalent interactions retain close together two entities formed by simple bond cleavages so that they are able to react unimolecularly (e.g., an incipient cation may isomerize) or bimolecularly (e.g., by hydrogen atom transfer),[7] supporting a similar proposal by Wendelboe, Bowen, and Williams.[8] In particular, both the isomerization of ionized butane to the

‡ Universitat de Barcelona.
§ E-mail: olivella@taga.qo.ub.es.
⊥ University of Texas Medical Branch.
⊗ Abstract published in *Advance ACS Abstracts,* September 15, 1996.
(1) Stockbauer, R.; Inghram, M. G. *J. Chem. Phys.* **1976**, *65*, 4081.
(2) Lifshitz, C.; Shapiro, M. *J. Chem. Phys.* **1967**, *46*, 4912.
(3) Wolkoff, P.; Holmes, J. L. *J. Am. Chem. Soc.* **1978**, *100*, 7346.
(4) Donchi, K. F.; Brownlee, R. T. C.; Derrick, P. J. *Chem. Soc., Chem. Commun.* **1980**, 1061.
(5) Gilman, J. P.; Hsieh, T.; Meisels, G. G. *J. Chem. Phys.* **1982**, *76*, 3497.
(6) Olivella, S.; Solé, A.; McAdoo, D. J.; Griffin, L. L. *J. Am. Chem. Soc.* **1994**, *106*, 11078.
(7) (a) Morton, T. H. *Tetrahedron* **1982**, *38*, 3195. (b) McAdoo, D. J. *Mass Spectrom. Rev.* **1988**, *7*, 363. (c) Bouchoux, G. *Adv. Mass Spectrom.* **1989**, *11*, 812. (d) Hammerum, S. In *Fundamentals of Gas Phase Ion Chemistry*; Jennings, K. R., Ed.; Kluwer Academic Publishers: Dordrecht, The Netherlands, 1990; pp 379−390. Bowen, R. D. *Acc. Chem. Res.* **1991**, *24*, 364. (e) Longevialle, P. *Mass Spectrom. Rev.* **1992**, *11*, 157. (f) McAdoo, D. J.; Morton, T. H. *Acc. Chem. Res.* **1993**, *26*, 295.

S0002-7863(96)00628-2 CCC: $12.00

isobutane radical cation and methane elimination from ionized butane were found to take place via an ion−neutral complex between a nonclassical H-bridged propyl cation and the methyl radical, which lies 15 kJ/mol *above* the sum of the energies of *sec*-propyl cation and methyl radical. Methane elimination from ionized isobutane also was found to take place via an ion−neutral complex between *sec*-propyl cation and methyl radical, lying 13 kJ/mol *below* the energy of its loosely bound components. These theoretical results were consistent with mass spectrometry experimental findings reported in the literature.

In light of the diversity of suggestions regarding the mechanism of the elimination of methane containing the internal methylene from ionized propane, the highly unusual nature of an alkane elimination from the middle of a carbon skeleton, and the specificity of the methane elimination, we undertook a theoretical study to try to answer the following questions: What is the ground-state equilibrium structure of ionized propane ($\mathbf{I}^{\bullet+}$)? Does an ion−neutral complex mediate the decomposition

$$\underset{\mathbf{I}^{\bullet+}}{\overset{\bullet+}{\lceil CH_3CH_2CH_3 \rceil}}$$

modes of $\mathbf{I}^{\bullet+}$ and, if so, what is its nature? Can methane elimination be specific and at the same time be complex-mediated rather than concerted? Does the carbon skeletal rearrangement of $\mathbf{I}^{\bullet+}$ precede the loss of methane bearing the central carbon atom and, if so, how does it take place? Why are the threshold energies for methane eliminations involving terminal and central carbon atoms within a few kJ/mol of each other? To answer these questions, we investigated the stationary points on the $C_3H_8^{\bullet+}$ ground-state potential energy surface (PES) most relevant to the $CH_3^{\bullet}$ and CH_4 losses from $\mathbf{I}^{\bullet+}$ by means of ab initio molecular orbital calculations. We report here the energetic and structural results of this theoretical investigation. The findings presented demonstrate that an ion−neutral complex mediates both the carbon skeletal rearrangement and the methane elimination from $\mathbf{I}^{\bullet+}$.

Computational Details

The geometries of the relevant stationary points on the $C_3H_8^{\bullet+}$ ground-state PES were located at the full (i.e., not frozen core) second-order Møller−Plesset perturbation theory[9] employing the split-valence d-polarized 6-31G(d) basis set.[10] The amount of spin contamination in the reference spin-unrestricted Hartree−Fock (UHF)[11] wave function was found to be very small; thus the expectation values of the $\hat{\mathbf{S}}^2$ operator were always very close to the value of 0.75 for a pure doublet state, i.e., in a range of 0.7586 to 0.7892. Some calculations were also carried out using (frozen core) quadratic configuration interaction with the singles and doubles (QCISD) method[12] employing the 6-31G(d) basis set. To characterize the stationary points as minima or as saddle points and to facilitate zero-point vibrational energy (ZPVE) corrections to the relative energies, the harmonic vibrational frequencies were obtained by diagonalizing the mass-weighted Cartesian force constant matrix. At the UMP2/6-31G(d) level, the force constant matrices were calculated from analytical second derivatives of the total energy, whereas at the QCISD/6-31G(d) level those matrices were calculated numerically by finite differences of analytical gradients. In order to predict more reliable ZPVE values, the raw UMP2/6-31G(d) harmonic vibrational frequencies were scaled by 0.93 to account for their average overestimation at this level of theory.[13]

Equilibrium structures were fully optimized within appropriate symmetry constraints using analytical gradient methods.[14] Starting geometries for the transition-structure optimizations were obtained by the usual reaction-coordinate method, the energy being minimized with respect to all other geometrical variables for successive increments in the reaction coordinate. The approximate transition structures located in this way were refined by minimizing the scalar gradient of the energy, using Schlegel's algorithm.[14] The optimized geometries were checked for the correct number of imaginary eigenvalues of the force constant matrix.

At geometries optimized using the UMP2/6-31G(d) wave function, the energies were recalculated using (frozen core) QCISD with the perturbative estimation of triples (QCISD(T)) method[12] employing the double d,p-polarized triple split-valence 6-311G(2d,2p) basis set.[15] In order to see if diffuse functions might be important in describing cation−molecule interactions, the QCISD(T) calculations were also carried out with the 6-311+G(2d,2p) basis set, which includes a single additional diffuse sp shell on heavy atoms only.[16] There was little difference in the energy changes calculated using the two basis sets and only the energies derived from the latter are reported. Our best relative energies correspond to the QCISD(T)/6-311+G(2d,2p) level together with the ZPVE correction calculated at the UMP2/6-31G(d) level. Unless otherwise noted, relative energies in the text refer to this overall level of theory.

Basis set superposition errors (BSSE) are expected to affect the computed interaction in electrostatically bound species.[17] However, it has been shown that these effects, although they tend to overestimate the ion−neutral complex stability relative to that of the completely separated components, are not very pronounced and do not exceed 4−8 kJ/mol.[18]

The charge and spin density distributions of the most relevant structures were analyzed within the framework of the topological theory of atoms in molecules[19] by means of the relaxed first-order electron density and spin density matrices obtained from UMP2 (full) gradient calculations with the 6-31G(d) basis set.[20]

All of the ab initio calculations described here were performed with the GAUSSIAN 92 and GAUSSIAN 94 program packages,[21] running on an IBM RS6000/58H workstation and on the IBM SP2 computer at the Centre de Supercomputacio de Catalunya (CESCA) in Barcelona. A locally modified version[22] of the PROAIM program[23] was employed in computations of Bader atomic charges and spin densities.

(8) Wendelboe, J. F.; Bowen, R. D.; Williams, D. H. *J. Am. Chem. Soc.* **1981**, *103*, 2333.
(9) (a) Møller, C.; Plesset, M. *Phys. Rev.* **1934**, *46*, 618. (b) Pople, J. A.; Binkley, J. S.; Seeger, R. *Int. J. Quantum Chem. Symp.* **1976**, *10*, 1.
(10) Hariharan, P. C.; Pople, J. A. *Theor. Chim. Acta* **1973**, *28*, 213.
(11) Pople, J. A.; Nesbet, R. K. *J. Chem. Phys.* **1954**, *22*, 571.
(12) Pople, J. A.; Head-Gordon, M.; Raghavachari, K. *J. Chem. Phys.* **1987**, *87*, 5968.
(13) (a) Hout, R. F.; Levi, B. A.; Hehre, W. J. *J. Comput. Chem.* **1982**, *3*, 234. (b) DeFrees, D. J.; McLean, A. D. *J. Chem. Phys.* **1985**, *82*, 333.
(14) Schlegel, H. B. *J. Comput. Chem.* **1982**, *3*, 214.
(15) Frisch, M. J.; Pople, J. A.; Binkley, J. S. *J. Chem. Phys.* **1984**, *80*, 3265.
(16) Hehre, W. J.; Radom, L.; Schleyer, P. v. R.; Pople, J. A. *Ab Initio Molecular Orbital Theory*; John Wiley: New York, 1986; pp 86−87.
(17) See, for example: (a) Urban, M.; Hozba, P. *Theor. Chim. Acta* **1975**, *36*, 215. (b) Ostlund, N. S.; Merrifield, D. L. *Chem. Phys. Lett.* **1976**, *39*, 612. (c) Bulski, H.; Chalasinski, G. *Theor. Chim. Acta* **1977**, *44*, 399. (d) Kolos, W. *Theor. Chim. Acta* **1979**, *51*, 219. (e) Leclercq, J. M.; Allavena, M.; Bouteilleur, Y. *J. Chem. Phys.* **1983**, *78*, 4606. (f) Hobza, P.; Zahradnik, R. *Int. J. Quantum Chem.* **1983**, *23*, 325. (g) Wells, B. H.; Wilson, S. *Chem. Phys. Lett.* **1983**, *101*, 429.
(18) (a) Latajka, Z.; Scheiner, S. *Chem. Phys.* **1985**, *98*, 59. (b) Postma, R.; Ruttink, P. J. A.; van Baar, B.; Terlouw, J. K.; Holmes, J. L.; Burgers, P. C. *Chem. Phys. Lett.* **1986**, *123*, 409.
(19) Bader, R. F. W. *Atoms in Molecules. A Quantum Theory*; Clarendon Press: Oxford, 1990.
(20) See, for example: Wiberg, K. B.; Hadad, C. M.; LePage, T.; Breneman, C. M.; Frisch, M. J. *J. Phys. Chem.* **1992**, *96*, 671.
(21) (a) Frisch, M. J.; Trucks, G. W.; Head-Gordon, M.; Gill, P. M. W.; Wong, M. W.; Foresman, J. B.; Johnson, B. G.; Schlegel, H. B.; Robb, M. A.; Replogle, E. S.; Gomperts, R.; Andres, J. L.; Raghavachari, K.; Binkley, J. S.; Gonzalez, C.; Martin, R. L.; Fox, D. J.; Defrees, D. J.; Baker, J.; Stewart, J. J. P.; Pople, J. A. *GAUSSIAN 92*; Gaussian, Inc.: Pittsburgh, PA, 1992. (b) Frisch, M. J.; Trucks, G. W.; Schlegel, H. B.; Gill, P. M. W.; Johnson, B. G.; Robb, M. A.; Cheeseman, J. R.; Keitth, T. A.; Petersson, G. A.; Montgomery, J. A.; Raghavachari, K.; Al-Laham, M. A.; Zakrzewski, V. G.; Ortiz, J. V.; Foresman, J. B.; Cioslowski, J.; Stefanov, A.; Nanayakkara, A.; Challacombe, M.; Peng, C. Y.; Ayala, P. Y.; Chen, W.; Wong, M. W.; Andres, J. L.; Replogle, E. S.; Gomperts, R.; Martin, R. L.; Fox, D. J.; Binkley, J. S.; Defrees, D. J.; Baker, J.; Stewart, J. J. P.; Head-Gordon, M.; Gonzalez, C.; Pople, J. A. *GAUSSIAN 94*; Gaussian, Inc.: Pittsburgh, PA, 1995.
(22) Mota, F., Universitat de Barcelona, unpublished work.

Table 1. Calculated Total Energies (hartrees) and Zero-Point Vibrational Energies (ZPVE, kJ/mol)[a] for MP2/6-31G(d) Optimized Structures

structure	point group	state	n.i.v.f.[b]	UMP2/6-31G(d)	QCISD[c]/6-311+G(2d,2p)	QCISD(T)[c]/6-311+G(2d,2p)	ZPVE
I	C_{2v}	$^1A_1$	0	−118.674 41	−118.843 97	−118.862 12	261
II	C_{2v}	$^2B_2$	0[d]	−118.279 91	−118.442 12	−118.460 23	247
III	C_s	$^2A'$	0	−118.279 06	−118.445 68	−118.461 90	246
IV	C_{2v}	$^1A_1$	0	−78.561 45	−78.661 93	−78.673 03	154
$CH_3^•$	D_{3h}	$^2A_2''$	0	−39.673 03	−39.741 28	−39.745 31	75
V	D_2	$^2B_1$	0	−77.926 51	−78.015 89	−78.024 10	123
CH_4	T_d	$^1A_1$	0	−40.337 04	−40.414 68	−40.420 05	113
VI	C_s	$^2A'$	1	−118.240 55	−118.408 90	−118.424 37	233
VII	C_s	$^2A'$	1	−118.240 60	−118.409 98	−118.425 59	233
VIII	C_s	$^2A'$	0	−118.247 95	−118.415 79	−118.432 26	233
IX	C_s	$^2A'$	1	−118.247 73	−118.416 58	−118.433 76	230
X	C_s	$^2A'$	0	−118.268 22	−118.437 25	−118.453 87	240
XI	C_1	^2A	1	−118.209 83	−118.380 11	−118.398 29	223

[a] Calculated using MP2/6-31G(d) vibrational frequencies, scaled by 0.93. [b] Number of imaginary vibrational frequencies. [c] In the frozen core approximation. [d] At the QCISD/6-31G(d) level it has 1 imaginary vibrational frequency.

Table 2. Calculated Relative Energies (kJ/mol) for MP2/6-31G(d)-Optimized Stationary Points on the $C_3H_8^{•+}$ Potential Energy Surface

stationary point	UMP2/6-31G(d)	QCISD[a]/6-311+G(2d,2p)	QCISD(T)[a]/6-311+G(2d,2p)	QCISD(T)[a]/6-311+G(2d,2p) + ZPVE	exp
III	0	0	0	0	
II	−2	9	4	5	
IV + $CH_3^•$	117	112	114	97	97[b]
V + CH_4	41	40	47	37	41[c]
VI	101	97	99	86	
VII	101	94	95	82	74[d]
VIII	82	78	78	65	
IX	82	76	74	58	
X	28	22	21	15	
XI	182	172	167	144	

[a] In the frozen core approximation. [b] Estimated from 0 K heats of formation.[42] [c] Estimated from 0 K heats of formation.[45] [d] Estimated from the appearance potential[46] for methane elimination from ionized propane and the propane adiabatic ionization potential.[42]

Table 3. Calculated Atomic Charges for MP2/6-31G(d)-Optimized Structures[a,b]

atom	**III**	**IV**	**VI**	**VII**	**VIII**	**IX**	**X**
C1	−0.100	−0.057	−0.048	−0.132	−0.077	−0.082	+0.011
C2	−0.079	−0.057	−0.048	+0.016	−0.077	−0.085	−0.019
C3	−0.100		−0.250	−0.259	−0.265	−0.261	−0.139
H1	+0.172	+0.245	+0.234	+0.188	+0.198	+0.189	+0.194
H2	+0.122	+0.217	+0.212	+0.188	+0.198	+0.189	+0.194
H3	+0.122	+0.217	+0.212	+0.240	+0.276	+0.281	+0.006
H4	+0.167	+0.217	+0.212	+0.216	+0.198	+0.189	+0.193
H5	+0.167	+0.217	+0.212	+0.216	+0.198	+0.189	+0.193
H6	+0.176		+0.088	+0.109	+0.117	+0.131	+0.126
H7	+0.176		+0.090	+0.109	+0.117	+0.131	+0.126
H8	+0.183		+0.088	+0.113	+0.117	+0.130	+0.117

[a] Determined from Bader population analysis of the UMP2(full)/6-31G(d) wave function. [b] Atom numberings refers to Figures 2−8.

Table 4. Calculated Atomic Spin Densities for MP2/6-31G(d)-Optimized Structures[a,b]

atom	**III**	**VI**	**VII**	**VIII**	**IX**	**X**
C1	0.039	0.010	0.042	0.043	0.079	0.556
C2	0.345	0.010	0.033	0.042	0.076	0.247
C3	0.489	0.979	0.906	0.878	0.797	0.187
H1	0.081	0.010	0.000	0.000	−0.001	−0.006
H2	0.006	0.000	0.000	0.000	−0.001	−0.006
H3	0.006	0.000	0.013	0.041	0.047	0.024
H4	0.009	0.000	0.004	0.000	−0.001	−0.006
H5	0.009	0.000	0.004	0.000	−0.001	−0.006
H6	0.003	−0.003	−0.001	0.000	0.001	0.004
H7	0.003	−0.003	−0.001	0.000	0.001	0.004
H8	0.010	−0.003	−0.002	0.000	0.001	0.001

[a] Determined from Bader population analysis of the UMP2(full)/6-31G(d) wave function. [b] Atom numberings refers to Figures 2 and 4−8.

Results and Discussion

The most relevant geometrical parameters of the optimized molecular structure are given in Figures 1−9 (bond lengths in Å and bond angles in deg), which are computer-generated plots of the UMP2/6-31G(d)-optimized geometries. The fully optimized geometries are available as supporting information. Total energies calculated at various levels of theory are given in Table 1, which includes the ZPVE computed from the scaled vibrational frequencies. Relative energies are collected in Table 2, together with experimental data derived from known heats of formation or appearance energy measurements. Finally, the total atomic charges and spin densities of the most relevant structures are shown in Tables 3 and 4, respectively.

A. Propane Radical Cation. For the purpose of illustrating the change in molecular geometry accompanying ionization, Figure 1 shows the equilibrium structure (**I**) of neutral propane optimized at the MP2/6-31G(d) level. Except for the more elongated C−H bonds, the geometry of **I** agrees very well with that obtained at the HF/6-31G(d) level.[24] We note the excellent agreement between the calculated C−C bond distance of 1.524

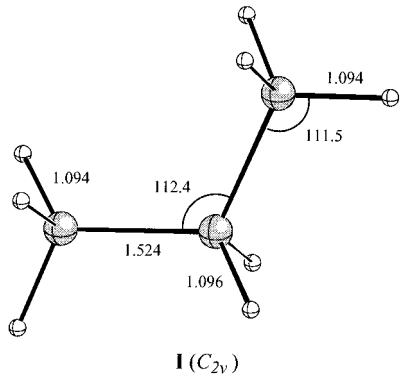

I (C_{2v})

Figure 1. MP2/6-31G(d)-optimized equilibrium structure of neutral propane.

(23) (a) Biegler-König, F. W.; Bader, R. F. W.; Tang, T.-H. *J. Comput. Chem.* **1982**, *3*, 317. (b) Bader, R. F. W.; Tang, T.-H.; Tal, Y.; Biegler-König, F. W. *J. Am. Chem. Soc.* **1982**, *104*, 946.

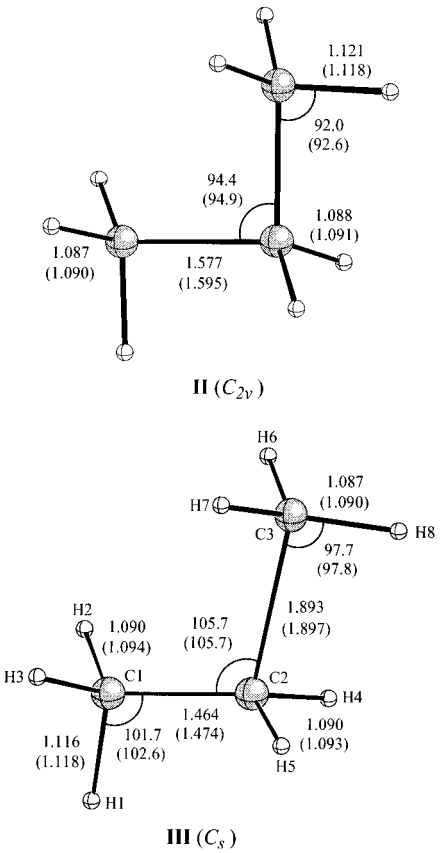

Figure 2. UMP2/6-31G(d)-optimized structures of the propane radical cation (QCISD/6-31G(d)-optimized geometrical parameters are given in parentheses).

Å and the experimental value of 1.526 Å.[24] As observed in previous theoretical studies,[25] the three highest occupied molecular orbitals of **1** (i.e., $6a_1$, $4b_2$, and $2b_1$) were found to be close in energy (within 0.3 eV). The equilibrium structure of $\mathbf{I}^{\bullet+}$ was first investigated in C_{2v} symmetry. In agreement with previous calculations of Lunell and co-workers,[26] we found that removal of an electron from the $4b_2$ orbital produces a radical cation in the $^2B_2$ state, which turned out to be the electronic ground state of $\mathbf{I}^{\bullet+}$ at the UMP2/6-31G(d) level. The optimized geometry of this state, **II** (Figure 2), shows that the C−C bond distances are 0.053 Å longer and the C−C−C bond angle is 18° smaller as compared with the equilibrium structure **I** calculated for the neutral parent molecule. The harmonic vibrational frequencies calculated for **II** indicated that it is a true local minimum on the UMP2/6-31G(d) PES. As was previously found by Bellville and Bauld[27] and Bouma and co-workers,[25] a C_s minimum with one long and one short C−C bond was located on the ground-state PES whose electronic wave function has $^2A'$ symmetry. At the UMP2/6-31G(d) level, the optimized geometry of this minimum, **III** (Figure 2), is higher in energy than **II** by only 2 kJ/mol. However, single-point QCISD and QCISD(T) calculations with the 6-311+G(2d,2p) basis set at the UMP/6-31G(d) optimized geometries showed that **III** is 9 and 4 kJ/mol, respectively, *less* energetic than **II**. For checking purposes, we carried out additional geometry optimizations of the electronic ground state of $\mathbf{I}^{\bullet+}$ in C_{2v} and C_s symmetries at the QCISD level of theory with the 6-31G(d) basis set. The most relevant geometrical parameters of the QCISD optimized structures are given in Figure 2, along with the UMP2/6-31G(d) optimized values. With the exception of the C−C bonds that are somewhat longer, the QCISD and UMP2 optimized geometries agree closely. At the QCISD/6-31G(d) level, the C_{2v} structure (**II**) is higher in energy than the C_s one (**III**) by 8 kJ/mol.[28] The calculated harmonic vibrational frequencies showed that **II** is a saddle point on the QCISD/6-31G(d) PES, while **III** is a true local energy minimum. The one imaginary frequency (317*i*) of **II** corresponds to a normal mode of b_2 symmetry, which leads to a shortening of one and the lengthening of the other C−C bond, i.e. to a distortion toward the C_s structure **III**. At the QCISD(T)/6-311+G(2d,-2p)//QCISD/6-31G(d) level the energy difference between **II** and **III** is calculated to be only 4 kJ/mol.[29] Inclusion of the ZPVE correction calculated from the unscaled QCISD/6-31G-(d) harmonic vibrational frequencies leads to an energy difference of only 3 kJ/mol at 0 K. This energy difference represents the barrier to interconversion of two equivalent structures **III**:

$$CH_3{-}CH_2{-}\overset{\bullet+}{C}H_2{-}CH_3 \rightleftharpoons CH_3{-}\overset{\bullet+}{C}H_2{-}CH_2{-}CH_3 \qquad (1)$$

Such an interconversion is clearly a facile process. At this point we note that recent density functional theory (DFT) calculations[30] (using the parametrization due to Vosko et al.[31] including nonlocal density gradient corrections by Becke[32] for the exchange functional and by Perdew[33] for the correlation part) performed with a polarized double-ζ basis set do not support the existence of a "long-bond" ground state $\mathbf{I}^{\bullet+}$ of lower symmetry than C_{2v}. To investigate whether the expected C_{2v} structure of $\mathbf{I}^{\bullet+}$ may be found as a minimum on a PES computed with a more accurate DFT method, B3-LYP (Becke's three-parameter nonlocal exchange hybrid functional[34] with the nonlocal correlation functional of Lee et al.[35]) geometry optimization and harmonic vibrational frequencies calculations with the 6-311G(d,p) basis were performed. Once again it was found that **II** is a saddle point on the B3-LYP/6-311G(d,p) PES, while **III** is a true local energy minimum. At the B3-LYP/6-311G(d,p) level, **II** was calculated to be higher in energy than **III** by only 4 kJ/mol.[36] In conclusion, at both the QCISD and B3-LYP levels of theory, the electronic ground-state of $\mathbf{I}^{\bullet+}$ is predicted to be a long-bond C_s structure.

The energy of **III** relative to that of **I** (Table 1), i.e., the calculated adiabatic ionization potential of **1**, is 10.74 eV. Experimental values range from 10.9[37] to 11.14[38] eV. On the other hand, the first vertical ionization potential of propane, determined as the difference in total energies (QCISD(T)/6-311+G(2d,2p)) of propane and ionized propane ($^2B_2$) (both calculations being performed at the optimum geometry **I**),[39] is 12.07 eV, compared with experimental values of 11.5[37] and 12.7 eV.[40]

(24) Hehre, W. J.; Radom, L.; Schleyer, P. v. R.; Pople, J. A. *Ab Initio Molecular Orbital Theory*; John Wiley: New York, 1986; p 168.
(25) Bouma, W. J.; Poppinger, D.; Radom, L. *Isr. J. Chem.* **1983**, *23*, 21.
(26) (a) Lunell, S.; Feller, D.; Davidson, E. R. *Theor. Chim. Acta* **1990**, *77*, 111. (b) Lunell, S.; Eriksson, L. A.; Huang, M.-B. *J. Mol. Struct. (THEOCHEM)* **1991**, *230*, 263.
(27) Bellville, D. J.; Bauld, N. L. *J. Am. Chem. Soc.* **1982**, *104*, 5700.
(28) QCISD/6-31G(d) energies in hartrees: −118.31323 (**II**) and −118.31627 (**III**).
(29) QCISD(T)/6-311+G(2d,2p)//QCISD/6-31G(d) energies in hartrees: −118.46038 (**II**) and −118.46177 (**III**).
(30) Eriksson, L. A.; Lunell, S.; Boyd, R. J. *J. Am. Chem. Soc.* **1993**, *115*, 6896.
(31) Vosko, S. H.; Wilk, L.; Nusair, M. *Can. J. Phys.* **1980**, *58*, 1200.
(32) Becke, A. D. *Phys. Rev. A* **1988**, *38*, 3098.
(33) Perdew, J. P. *Phys. Rev. B* **1986**, *33*, 8822; **1986**, *34*, 7406.
(34) Becke, A. D. *J. Chem. Phys.* **1993**, *98*, 5648.
(35) Lee, C.; Yang, W.; Parr, R. G. *Phys. Rev. B* **1988**, *37*, 785.
(36) B3-LYP/6-311G(d,p) energies in hartrees: −118.78448 (**II**) and −118.78598 (**III**).
(37) Bieri, G.; Burger, F.; Heilbronner, E.; Maier, J. P. *Helv. Chim. Acta* **1977**, *60*, 2213.
(38) Nicholson, A. J. C. *J. Chem. Phys.* **1965**, *43*, 1171.
(39) QCISD(T)/6-311+G(2d,2p)//QCISD/6-31G(d) energy in hartrees: −118.41842.

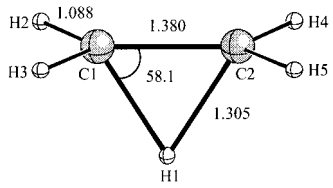

IV (C_{2v})

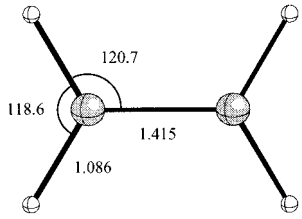

V (D_2)

Figure 3. MP2/6-31G(d)-optimized equilibrium structure of the H-bridged ethyl cation (**IV**) and UMP2/6-31G(d)-optimized equilibrium structure of the ethene radical cation (**V**).

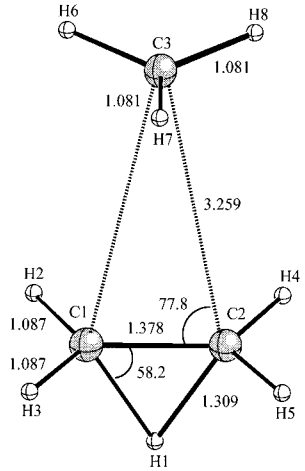

VI (C_s)

Figure 4. UMP2/6-31G(d)-optimized transition structure involved in the carbon skeletal rearrangement of propane radical cation.

B. Loss of $CH_3^\bullet$ from Ionized Propane. We elongated the long C−C bond of **III** systematically in steps of 0.1 Å by optimizing all other geometry parameters to simulate the minimum energy reaction path (MERP) for $CH_3^\bullet$ elimination. The increase of the C2−C3 distance caused a simultaneous lengthening of the *anti* C−H bond accompanied by the displacement of the H1 hydrogen atom toward the C2 carbon atom, while the energy increased steadily. This path led to the dissociation of $\mathbf{I}^{\bullet+}$ to $C_2H_5^+$ and $CH_3^\bullet$. In agreement with previous theoretical investigations at more sophisticated ab initio levels,[41] our MP2/6-31G(d) calculations predict a H-bridged equilibrium structure for $C_2H_5^+$ (**IV**, Figure 3). It is worth noting that the C−C bond length and the distance between the bridged hydrogen atom and the carbon atoms calculated for **IV** are in excellent agreement with the values of 1.380 and 1.309 Å, respectively, predicted by recent coupled-cluster singles and doubles calculations using a triple-ζ double polarization basis set.[41c] At the UMP2/6-31G(d) level, the sum of the energies of the separated fragments, $C_2H_5^+$ and $CH_3^\bullet$, lies 117 kJ/mol above the energy of **III**. At the QCISD(T)/6-311+G(2d,2p) level, this dissociation energy is calculated to be 114 kJ/mol. The ZPVE correction reduces the predicted (0 K) dissociation energy to the value of 97 kJ/mol, which is in excellent agreement with the experimental estimate of 97 kJ/mol determined from 0 K heats of formation.[42]

C. Carbon Skeletal Rearrangement of the Ionized Propane. Starting from structure **III** with the long C2−C3 bond distance stretched to 2.96 Å, an extensive grid search using this distance and the C1−C2−C3 bond angle as reaction coordinates while maintaining the initial C_s symmetry led to the approximate location of a saddle point at C2−C3 = 3.25 Å and C1−C2−C3 = 78°. The structure located in this way was refined by minimizing the scalar gradient of the energy using Schlegel's algorithm. The resulting optimized structure, **VI** (Figure 4), was characterized as a true transition structure by checking that it had only one imaginary harmonic vibrational frequency. The atomic displacements associated to the one imaginary frequency (145*i*) of **VI** consisted mainly of a combined closure (or opening) of the C1−C2−C3 and H1−C1−C2 angles. Further decrements of the C1−C2−C3 angle in **VI** yielded a smooth path leading to a structure akin to **III**, showing one long (C3−C1) and one short (C1−C2) bond. Therefore, **VI** is a transition structure for the carbon skeletal rearrangement of $\mathbf{I}^{\bullet+}$:

$$CH_3-\mathbf{C}H_2-CH_3\rceil^{\bullet+} \rightleftharpoons CH_3-CH_2-\mathbf{C}H_3\rceil^{\bullet+} \qquad (2)$$

At the UMP2/6-31G(d) and QCISD(T)/6-311+G(2d,2p) levels of theory, **VI** lies 101 and 99 kJ/mol, respectively, above **III**. Inclusion of the ZPVE correction in the latter value leads to an energy of activation at 0 K of 86 kJ/mol for the degenerate rearrangement of eq 2.

The long C1−C3 and C2−C3 distances (3.259 Å) in **VI**, along with the fact that the CH_3 and C_2H_5 parts show geometries nearly identical to the equilibrium structures calculated for the isolated methyl radical and H-bridged ethyl cation **IV** (Figure 3), indicate that these entities are loosely bound in **VI**. Furthermore, the charge and spin density distributions (Tables 3 and 4) show that the sum of the total atomic charges of the ethyl unit (+0.985) accounts for nearly the 99% of the positive charge of **VI**, whereas the sum of the total spin densities of the methyl unit (0.970) accounts for the 97% of the unpaired electron population of **VI**. Therefore, on the basis of the molecular geometry and the distribution of the total atomic charges and spin densities, **VI** can be viewed as an ion−neutral complex between the H-bridged ethyl cation and the methyl radical. Since the dissociation energy of **III** to $C_2H_5^+$ and $CH_3^\bullet$ is calculated to be 97 kJ/mol and **VI** is predicted to lie 86 kJ/mol above **III**, it turns out that **VI** is stabilized by 11 kJ/mol toward decomposition to its loosely bound components.

D. Elimination of CH_4 from Ionized Propane. The equilibrium structure (**V**) calculated for the ethene radical cation produced in the methane elimination from $\mathbf{I}^{\bullet+}$ is displayed in Figure 3. The torsional angle between the two CH_2 groups of **V** is predicted to be 13.0°. This value is close to the torsional angle of 12.3° calculated at the UMP2/6-311++G(2d,2p) level by Lunell and co-workers,[26b] but deviates 12° from the estimated experimental value of 25°, based on an analysis of the vibrational structure in UV absorption and photoelectron spectra.[44] On the other hand, the endothermicity of 37 kJ/mol at 0 K predicted for the reaction **III** → **V** + CH_4 compares

(40) Stockbauer, R.; Inghram, M. G. *J. Chem. Phys.* **1971**, *54*, 2242.

(41) (a) Ruscic, B.; Berkowitz, J.; Curtis, L. A.; Pople, J. A. *J. Chem. Phys.* **1989**, *91*, 114. (b) Klopper, W.; Kutzelnigg, W. *J. Phys. Chem.* **1990**, *94*, 5625. (c) Perera, S. A.; Bartlett, R. J.; Schleyer, P. v. R. *J. Am. Chem. Soc.* **1995**, *117*, 8476.

(42) $\Delta H_f(C_2H_5^+)$ = 914 (ref 43), $\Delta H_f(CH_3^\bullet)$ = 149 (ref 43), and $\Delta H_f(CH_3CH_2CH_3^{\bullet+})$ = 966 kJ/mol at 0 K. The latter value was obtained combining $\Delta H_f(CH_3CH_2CH_3)$ = −90 kJ/mol at 0 K (Traeger, J. C.; Hudson, C. E.; McAdoo, D. J. *J. Phys. Chem.* **1988**, *92*, 1519) and the propane adiabatic ionization potential of 10.95 ± 0.05 eV (ref 43).

(43) Lias, S. G.; Bartmess, J. E.; Liebman, J. B.; Holmes, J. L.; Levin, R. D.; Mallard, W. G. *J. Phys. Chem. Ref. Data* **1988**, *17*, 168.

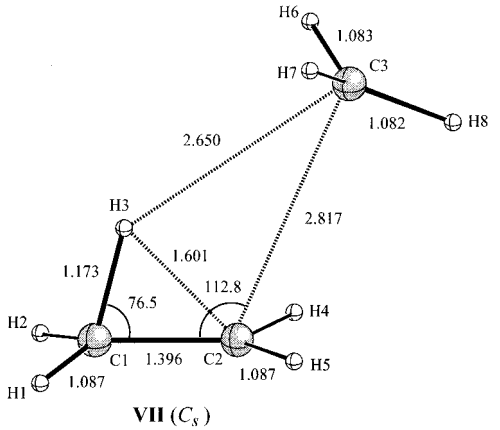

Figure 5. UMP2/6-31G(d)-optimized transition structure connecting propane radical cation **III** and the ion−neutral complex **VIII**.

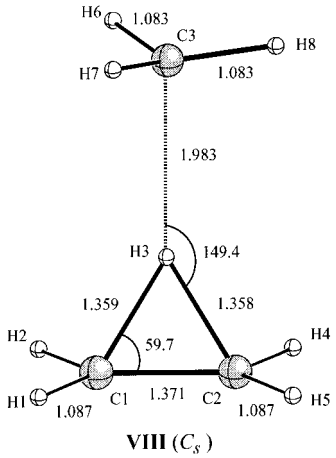

Figure 6. UMP2/6-31G(d)-optimized equilibrium structure of the ion−neutral complex between methyl radical and H-bridged ethyl cation.

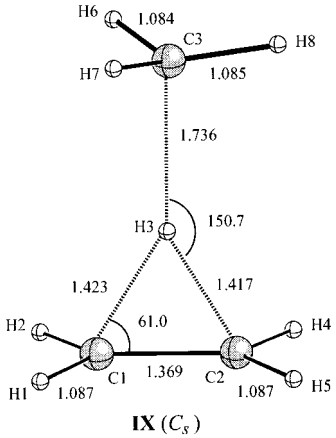

Figure 7. UMP2/6-31G(d)-optimized transition structure for the transfer of the bridging hydrogen atom of $C_2H_5^+$ to the $CH_3^\bullet$ partner in the ion−neutral complex **VIII**.

well with the relative enthalpy of 41 kJ/mol for $\mathbf{I}^{\bullet+}$ with respect to ethene radical cation and methane, estimated from 0 K heats of formation.[45]

The methane elimination from $\mathbf{I}^{\bullet+}$ was found to proceed in three steps. Starting from **III**, the formation of the fragments $CH_4 + C_2H_4^{\bullet+}$ implies a hydrogen atom transfer from C1 to C3 accompanied by the scission of the C2−C3 bond. Therefore, we investigated the elongation of the latter bond combined with the shortening of the C3−H3 distance in **III**. This reaction path led to the approximate location of a saddle point at C2−C3 = 2.81 Å and C3−H3 = 2.65 Å. The structure located in this way was optimized using Schlegel's algorithm. The resulting stationary point, **VII** (Figure 5), was characterized as a true transition structure by checking that it had only one imaginary harmonic vibrational frequency. The one imaginary frequency (607*i*) corresponded chiefly to the simultaneous lengthening of the C1−H3 and C2−C3 bonds combined with a shifting of the H3 hydrogen atom toward the C2 carbon atom. The H3−C1−C2 bond angle of 76.5°, the C1−C2 bond distance of 1.396 Å, and the C1−H3 bond distance of 1.173 Å (Figure 5) indicate that the ethyl part of the transition structure **VII** looks like a distorted classical ethyl cation.[41] Furthermore, an analysis of the charge and spin density distributions (Tables 3 and 4) reveals that the sum of the total atomic charges of the ethyl part (+0.932) accounts for more than 93% of the positive charge of **VII**, whereas the sum of the total spin densities of the methyl part (0.902) accounts for more than 90% of the unpaired electron population of **VII**. Therefore, the transition structure **VII** can be viewed as a distorted classical ethyl cation coordinated to the methyl radical. The energy of this complex (Table 2) is calculated to be 82 kJ/mol above **III** and 15 mJ/mol below that of H-bridged ethyl cation plus methyl radical.

Further increments of the C2−C3 bond in **VII** led to a continuous decrease of the H3−C1−C2 angle while the C3 carbon atom was progressively shifted to the H3 hydrogen atom. This reaction path led to the stationary point **VIII** (Figure 6) showing C1−C3 and C2−C3 distances of 3.232 and 3.227 Å, respectively. The force constant matrix of **VIII** turned out to have only positive eigenvalues, the lowest harmonic vibrational frequency (5 cm^{-1}) corresponding to a rotation of the methyl unit about the C3−H3 axis. It is worth noting that the C1−H3 and C2−H3 distances in **VIII** are 0.054 and 0.053 Å longer, respectively, than in the equilibrium structure **IV** optimized for the isolated $C_2H_5^+$ ion. This seems to indicate that there is a loose C3···H3 bonding interaction between the C_2H_5 and CH_3 parts of this structure. Regarding the charge and spin density distributions (Tables 3 and 4), it is noteworthy that the sum of the total atomic charges of the ethyl moiety (+0.914) accounts for nearly 91% of the positive charge of **VIII**, whereas the sum of the total spin densities of the methyl unit (0.878) accounts for nearly 88% of the unpaired electron population of **VIII**, indicating a weak (≈0.1 e^-) electronic charge transfer from the methyl radical to the H-bridged ethyl cation in **VIII**. Consequently, the molecular geometry and the distribution of the total atomic charges and spin densities suggest that **VIII** can be regarded as another configuration of the methyl−H-bridged ethyl complex **VI** in which the carbon atom of the methyl partner is loosely bound to the bridging hydrogen atom of the ethyl partner. At the UMP2/6-31G(d) and QCISD(T)/6-311+G(2d,-2p) levels of theory, the energy of complex **VIII** is calculated to be 35 and 36 kJ/mol, respectively, lower than that of its separated components, $C_2H_5^+$ and $CH_3^\bullet$. Inclusion of the ZPVE correction in the latter value leads to a stabilization energy of **VIII** toward decomposition into these fragments of 32 kJ/mol at 0 K.

The second step of the methane elimination from $\mathbf{I}^{\bullet+}$ was found to involve a hydrogen atom transfer between the methyl and the H-bridged ethyl partners of the ion−neutral complex **VIII**. Since this implies the formation of a covalent bond, the two partners of **VIII** should come much closer together. In fact, the C3−H3 distance of structure **VIII** (1.983 Å) is shortened to 1.736 Å in the transition structure **IX** (Figure 7) found for the hydrogen atom transfer. The normal mode associated with the single imaginary vibrational frequency of

(44) Merer, A. J.; Schoonveld, L. *Can. J. Phys.* **1969**, *47*, 1731.

(45) $\Delta H_f(CH_2{=}CH_2^{\bullet+}) = 1074$ (ref 43), $\Delta H_f(CH_4) = -67$ (ref 43), and $\Delta H_f(CH_3CH_2CH_3^{\bullet+}) = 966$ kJ/mol at 0 K. For the latter value see ref 42.

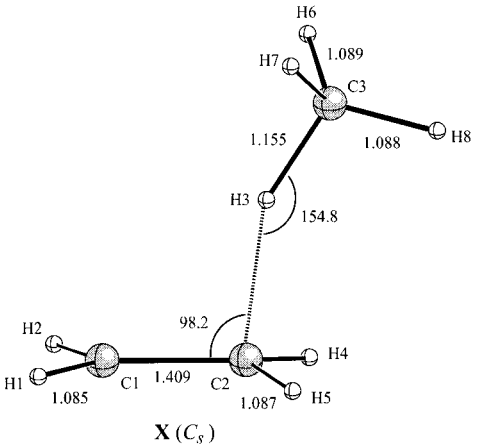

X (C_s)

Figure 8. UMP2-6-31G(d)-optimized equilibrium structure of the ion−neutral complex between ethene radical cation and methane.

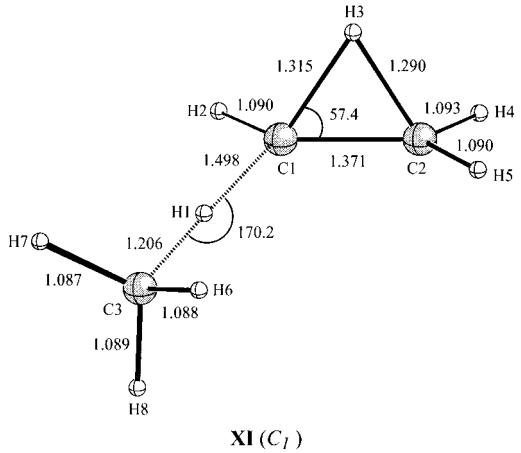

XI (C_1)

Figure 9. UMP2/6-31G(d)-optimized transition structure for the transfer of a nonbridging hydrogen atom of $C_2H_5^+$ to the $CH_3^\bullet$ partner in the ion−neutral complex **VIII**.

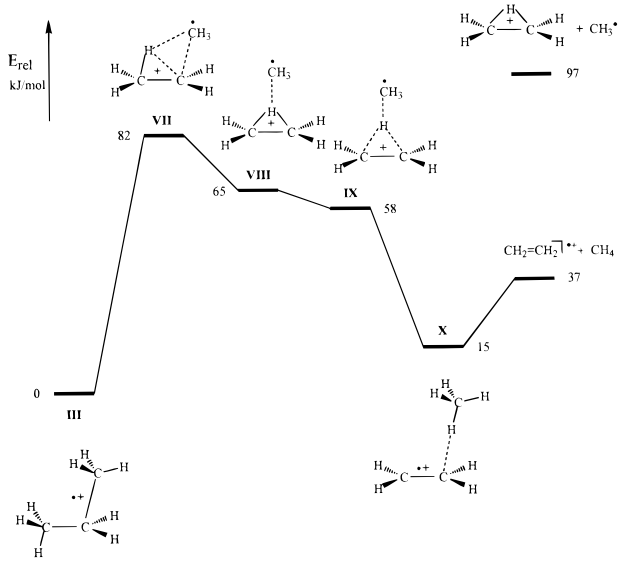

Figure 10. Schematic potential energy profile showing the methane elimination from ionized propane (**III**). Energy values obtained from the ZPVE-corrected QCISD/6-311+G(2d,2p) energies relative to that of **III**.

IX (272*i* cm^{-1}) is dominated by a shortening of the C3−H3 distance combined with a lengthening of the C1−H3 and C2−H3 distances. Regarding the charge and spin density distributions (Tables 3 and 4), it is noteworthy that the sum of the total atomic charges of the ethyl unit (+0.870) accounts for 87% of the positive charge of **IX**, whereas the sum of the total spin densities of the methyl unit (0.800) accounts for 80% of the unpaired electron population of **IX**. This indicates a weak electronic charge transfer from the methyl radical partner to the H-bridged ethyl cation in the transition structure **IX**. It can be seen from Table 2 that at the UMP2/6-31G(d) level there is an energy barrier of less than 1 kJ/mol associated to the hydrogen transfer process in **VIII**. However, at the QCISD(T)/6-311+G-(2d,2p) level of theory, **IX** is calculated to lie 4 kJ/mol *below* **VIII**. Since in this region the PES appears to be very flat, a meaningful evaluation of the relative energies of **VIII** and **IX** at a given level of theory should be done using the geometries optimized at the same level. Due to the prohibitive computational cost involved, the geometry re-optimization of these structures at the QCISD(T)/6-311+G(2d,2p) level was not attempted in the present study. These difficulties do not influence our determination of the overall energy barrier to methane elimination from **III**, as that barrier is the one for the first step.

A geometry re-optimization of **IX**, slightly modified according to the normal mode of the single imaginary vibrational frequency, with the appropriate sign, led to a local minimum (**X**, Figure 8) which appears to be an ion−neutral complex between the ethene radical cation and methane. Thus the geometrical parameters of the C_2H_4 part of structure **X** are nearly identical to those of the calculated equilibrium structure for the isolated ethene radical cation **V**, while the C3−H3 bond of the CH_4 part is 0.065 Å longer than in the calculated equilibrium structure for the isolated methane (1.090 Å). The charge and spin density distributions (Tables 3 and 4) show that the sum of the total atomic charges (+0.766) and the sum of the total spin densities (0.779) of the ethene unit account for nearly 77% of the positive charge and unpaired electron population of **X**. Therefore, there is a significant (≈0.2 e^-) electronic charge transfer from the ethene radical cation partner to the methane in the complex **X**. This complex is stabilized by 22 kJ/mol toward decomposition into $C_2H_4^{\bullet+}$ and CH_4. Since BSSE are expected to affect the computed interaction between the $C_2H_4^{\bullet+}$ and CH_4 partners in the complex **X**, this stabilization energy value should be taken with caution.

The above findings indicate that **IX** is the transition structure for the bridging hydrogen atom transfer between the ion−neutral complexes **VIII** and **X**. For the sake of completeness, the transfer of one of the peripheral hydrogen atoms of $C_2H_5^+$ to the $CH_3^\bullet$ partner in the ion−neutral complex **VIII** was also studied. For instance, the H1 atom transfer was found to take place through the transition structure **XI** (Figure 9). It is worth noting that the C3−H1 and C1−H1 distances (1.206 and 1.498 Å, respectively) in **XI** indicate a covalent binding of this transition structure. The normal mode associated with the single imaginary vibrational frequency of **XI** (801*i* cm^{-1}) corresponds chiefly to a shortening of one of these two C−H bonds and a lengthening of the other one. The energy of the saddle point **XI** is predicted to be 86 kJ/mol higher than that of **IX**. It can be concluded, therefore, that the transfer of a hydrogen atom other than the bridging hydrogen of $C_2H_5^+$ to the $CH_3^\bullet$ partner in the ion−neutral complex **VIII** is very unlikely.

Finally, the formation of the products **V** + CH_4 implies a simple separation of the two components of the complex **X**. UMP2/6-31G(d) calculations of the corresponding MERP showed a smooth increase of the potential energy until it reaches the separated products. Consequently, it appears that no reverse activation energy is associated to this dissociation. Figure 10 summarizes the potential energy profile calculated at the QCISD(T)/6-311+G(2d,2p)+ZPVE level for the methane elimination from **III**. The activation energy at 0 K for the overall

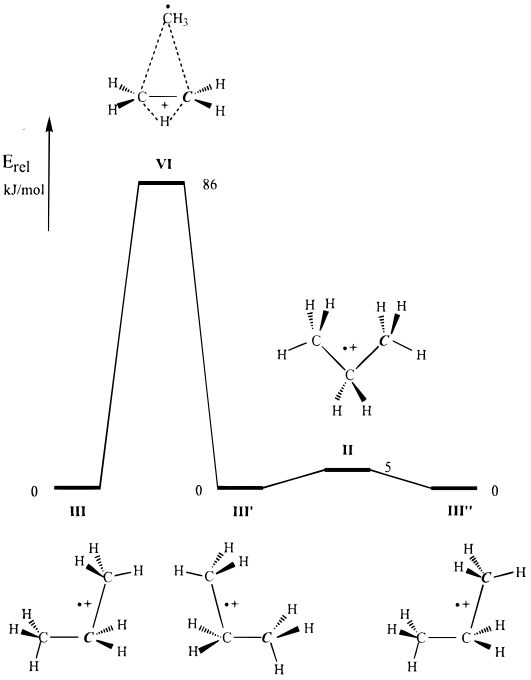

Figure 11. Schematic potential energy profile showing the carbon skeletal rearrangement of ionized propane (**III**) and the subsequent conversion of the rearranged radical cation (**III′**) to an equivalent structure (**III″**) which can eliminate methane containing the central carbon atom. Energy values obtained from the ZPVE-corrected QCISD/6-311+G(2d,2p) energies relative to that of **III**.

reaction via the rate-determining transition structure **VII** is predicted to be 82 kJ/mol, which is somewhat above the critical energy of 74 kJ/mol (0.77 eV) determined as the difference between the appearance potential of 11.72 ± 0.02 eV for the CH_4 elimination from $\mathbf{I}^{\bullet+}$ measured by Chupka and Berkowitz[46] and the recommended propane adiabatic ionization potential of 10.95 ± 0.05 eV.[42]

The intriguing observation that a small amount (≈11%) of all methane loss from ionized propane-*2*-^{13}C includes the central carbon atom is readily explained if one assumes that the carbon skeletal rearrangement of eq 2 precedes the elimination of methane involving the central carbon atom. Figure 11 provides a schematic potential energy profile, calculated at the QCISD-(T)/6-311+G(2d,2p)+ZPVE level, showing the two-step process required to generate a rearranged radical cation (i.e., **III″**) which can eliminate methane bearing the central carbon atom. Since the calculated overall activation energy of this isomerization (86 kJ/mol) is 4 kJ/mol higher than the calculated value (82 kJ/mol) for the subsequent methane elimination from the rearranged radical cation (see Figure 10), the carbon skeletal rearrangement is the rate-determining step for the methane elimination involving the central carbon atom. At this point we note that the predicted energy difference of 4 kJ/mol between the transition structures **VI** and **VII** is much lower than the measured[5] difference of 0.22 eV (21 kJ/mol) between the appearance potentials of the CH_4 and $^{13}CH_4$ losses from ionized propane-*2*-^{13}C. However, this discrepancy is likely due to kinetic and competive shifts and the combination of the uncertainties in all of the results. The complex-mediated elimination from and isomerization of $\mathbf{I}^{\bullet+}$ are similar to carbon skeletal rearrangements and alkane eliminations that occur in larger alkane radical cations[6,8,47] demonstrating further generality of such processes.

(46) Chupka, W. A.; Berkowitz, J. *J. Chem. Phys.* **1967**, *47*, 2921.
(47) Traeger, J. C.; Hudson, C. E.; McAdoo, D. J. *J. Am. Soc. Mass Spectrom.* **1996**, *7*, 73.

In summary, the present theoretical calculations reveal that the unusual features of the dissociations of $\mathbf{I}^{\bullet+}$ stem from the intermediacy of an ethyl ion−methyl radical complex. The specificity of the methane elimination arises from abstraction of the bridging hydrogen atom in a methyl−H-bridged ethyl complex in which the bridging hydrogen atom originates from a methyl of $\mathbf{I}^{\bullet+}$. Thus, this reaction is not concerted, as might be concluded from its specificity, so specificity in an H-transfer does not always rule out an ion−neutral complex intermediate. A concerted 1,2-elimination would be symmetry-forbidden in the Woodward−Hoffman sense;[48] passage through an ion−neutral complex enables the system to bypass the high-energy barrier that would be associated with a symmetry-forbidden, concerted process.

The specificity of methane elimination[1,5] also demonstrates that H-transfer in **VIII** is strongly favored over return to **III**, as 50% of such collapses would interchange the positions of the carbon atoms in $\mathbf{I}^{\bullet+}$, producing a repositioning of isotopic labels that clearly does not occur at the threshold for methane elimination. Carbon skeletal isomerization of $\mathbf{I}^{\bullet+}$ by way of ion−neutral complexes does occur, but only as a minor, higher energy process through a different configuration of the complex (e.g., **VI**). At the threshold for attaining **VIII**/**IX** it is clear that return to **III** does not compete with methane elimination. This is very surprising, as **VIII** should be able to return to **III**, the lowest energy point on the PES, by the pathway whereby it forms from $\mathbf{I}^{\bullet+}$. We rationalize its not doing so by relating the experimentally measured thresholds for the dissociations of $\mathbf{I}^{\bullet+}$ and our theoretical description of the PES as follows. Simple methane elimination at threshold occurs because the lowest energy trajectories for moving the methyl radical around the ethyl cation go near the bridging hydrogen atom. We suggest that the covalent bonding between the C3 and H3 atoms in **VIII** makes H-transfer-methane elimination from there much faster than return to **III**. A methyl group can move from one carbon of the ethyl group to the other only at higher energies at which it can do so without going near the bridging hydrogen atom. Thus the contours of the $C_3H_8^{\bullet+}$ ground-state PES are such that at the threshold for methane elimination the methyl radical partner of the ion−neutral complex is directed to the hydrogen atom it will abstract without being able to move freely around the ethyl cation partner. We know of no previous demonstration of a confined path from a ground state ion to the transition state for reaction between the partners in an ion−neutral complex.

Conclusions

Our computational exploration of the $C_3H_8^{\bullet+}$ ground-state potential energy surface in the regions concerning the $CH_3^{\bullet}$ and CH_4 losses from ionized propane reveals several important points:

(1) At the QCISD/6-31G(d) level of theory, the equilibrium structure of the ground state propane radical cation is predicted to be a C_s structure showing a long C−C bond of 1.897 Å and a somewhat short C−C bond of 1.474 Å. The interconversion between the two equivalent structures takes place via a C_{2v} transition structure showing two C−C bonds of 1.595 Å and involves an activation energy of about 5 kJ/mol.

(2) The carbon skeletal rearrangement of the propane radical cation takes place via a transition structure consisting of the methyl radical coordinated to the nonclassical H-bridged ethyl cation. This ion−neutral complex lies about 11 kJ/mol below the calculated energy of the dissociation fragments H-bridged ethyl cation plus methyl radical.

(48) Williams, D. H. *Acc. Chem. Res.* **1977**, *10*, 280.

(3) The methane elimination from ionized propane proceeds in three steps. The first one involves the formation of another configuration of the methyl−H-bridged ethyl complex, lying 32 kJ/mol below the energy of its separated components, in which the carbon atom of the methyl partner is loosely bound to the bridging hydrogen atom of the ethyl partner. This elementary reaction is the rate-determining step of the methane elimination from ionized propane and is characterized by a transition structure lying 15 kJ/mol below the thermochemical threshold for methyl radical loss, which looks like a methyl radical coordinated to a distorted classical ethyl cation. The second step implies the transfer of the bridging hydrogen atom from the ethyl partner to the methyl partner in the methyl−H-bridged ethyl complex intermediate with a negligible energy barrier, yielding an ion−neutral complex between the ethene radical cation and methane lying about 22 kJ/mol below its separated components. Finally, the formation of the products ethene radical cation plus methane implies a simple separation of the two components of the latter complex, and thus no reverse activation energy is associated to this dissociation.

(4) The specificity of the methane elimination arises from abstraction of the bridging hydrogen atom in the methyl−H-bridged ethyl complex in which the bridging hydrogen atom originates from a methyl of the propane radical cation.

(5) The carbon skeletal rearrangement is predicted to precede the elimination of methane from ionized propane involving the central carbon atom. This degenerate rearrangement is calculated to be the rate-determining step of the overall process leading to methane loss bearing the central carbon atom of the propane radical cation.

Acknowledgment. This paper is dedicated to Professor Juan Bertran, on the occasion of his 65th birthday. The work in Barcelona was supported by the Spanish DGICYT (Grant PB92-0796-C02-01). We acknowledge the CESCA for generous allocations of computing time.

Supporting Information Available: Cartesian coordinates of all structures reported in this paper (6 pages). See any current masthead page for ordering and Internet access instructions.

JA9606283